

International Journal of Control Theory and Applications

ISSN : 0974-5572

© International Science Press

Volume 10 • Number 34 • 2017

Wind Power Induced Inter-Area Oscillations PSS Performances

Ikram NACEF¹, Khadija BEN KILANI¹ and Mohamed ELLEUCH¹

¹ University of Tunis El Manar - ENIT- LSE

E-mail: ikramnacef28@gmail.com; khadijakilani@yahoo.fr; mohamed.elleuch@enit.utm.tn

Abstract: This paper addresses the issue of inter-area oscillations induced by wind power and their control by standard power system stabilizers. The purpose is twofold: first it is demonstrated that specific wind profiles may induce inter-area oscillations by the general forced oscillation mechanism. Second, power system stabilizer performances are assessed for their control and damping of the wind induced oscillations. Methodologically, the wind power output is frequency-analyzed by the power spectral density and the general forced oscillation mechanism is used in search for a correlation between the wind power spectrum and the inter-area oscillation frequencies indicated by modal analysis. The study is applied on a four-machine two areas power system. The results demonstrate the presence of wind power induced inter-area forced oscillations. Power system stabilizers performances depend on the wind profiles.

Keywords: Wind power fluctuation, inter-area oscillation, linear analysis, general forced oscillation, Fast Fourier Transform, power system stabilizer.

1. INTRODUCTION

Inter area oscillations are phenomena characterizing synchronously interconnected wide areas power systems [1]. They depend on the characteristics of the synchronous generators, the topology of the power system and its operating initial conditions [2]. They imply interactions among large groups of generating units, with low frequencies ranging from 0.1 Hz to 0.8 Hz. Their presence on the power network can limit the transmission capability of the grid and may endanger the dynamic stability of power systems [3].

Power system operators have long been seeking to understand the nature of these oscillations and their mechanism of excitation. Inter area oscillations characterize weakly connected systems suffering from negative damping properties. However, recent works [4] have reported sustained oscillations being observed in power systems not demonstrating poor damping characteristics. The general forced oscillation (GFO) mechanism has been proposed in [two paper GFO] to justify such sustained oscillations. Physically, forced oscillations in power systems may originate from cyclic loads [5-6], turbo-pressure pulsations [7], pressure fluctuations in hydraulic turbine draft tubes [8], and wind power fluctuations [9-10]. The authors in [11] have shown that the variability and the randomness of wind power generation inject more random components in the grid, and may excite low frequency oscillations. In [12], the effect of power fluctuations of fixed-speed wind farm in the Northern Ireland power system on the inter-area oscillations was investigated. The authors proved that there is a correlation

between the inter-area oscillation and the wind power output in the Irish power system. In [13], the general forced oscillation mechanism GFO has been applied to study the inter-area oscillations observed on the power grid of China. It has been proved that the wind power fluctuations have a high probability to induce the observed inter-area oscillations where the power spectral density of the wind power covers the frequency of the inter-area oscillation modes.

For the wind power output, it depends on the wind speed profiles which may be a simple ramp, a wind gust, a high turbulence or a composite model. From a control point of view, the inter-area oscillation damping depends on their frequencies and on their excitation mechanism, namely the wind profile, and the system operating conditions. Among wind power induced oscillations, the forced ones are of high interest because they are sustained and their control may not be achieved by standards power system stabilizers (PSS). Power system controls especially PSSs may or not be able to damp the inter-area oscillations induced by the various wind profiles. In the above context, their performances ought to be studied.

The purpose of this paper is twofold: first it is demonstrated that specific wind profiles may induce inter-area oscillations by the general forced oscillation mechanism. Second, power system stabilizer performances are assessed for their effectiveness in damping the wind power induced oscillations. Methodologically, the wind power output is frequency-analyzed by the power spectral density and the general forced oscillation mechanism is used in search for a correlation between the wind power spectrum and the inter-area oscillation frequencies indicated by modal analysis. The study is applied on a four-machine two areas power system. The results demonstrate the presence of wind power induced inter-area forced oscillations. Power system stabilizers performances are tested for their effectiveness in control and damping of wind power induced inter-area oscillations.

2. THE CONCEPT OF FORCED OSCILLATION

Generally, forced oscillations are investigated in time domain [19]. However, in the case of random stochastic excitations, time domain analysis may be inappropriate. Thus, we investigate the mechanism of forced oscillation in the frequency domain. There are two types of forced oscillations: Special forced oscillations (SFO), General forced oscillations (GFO).

(a) *Special forced oscillation*: The SFO mechanism indicates that forced oscillations in power systems may be caused by a continuous periodic perturbation [15]. The input excitation is a single frequency. When the frequency of the excitation source is equal to or near the natural oscillation frequency, the system resonance will be induced, resulting in forced oscillations. Assuming a continuous sine excitation applied on a synchronous generator, the rotor swing equation is written as follows:

$$H \frac{d^2 \Delta \delta}{dt^2} + D \frac{d \Delta \delta}{dt} + K_s \Delta \delta = F_0 \sin(\omega t) \quad (1)$$

where H , D , K_s and δ are the inertia constant, the damping coefficient, the synchronizing coefficient and the rotor angle, respectively. The amplitude of forced oscillations can be expressed as:

$$B = \frac{F_0 / K_s}{\sqrt{(1 - v^2)^2 + (2\zeta v)^2}} \quad (2)$$

where ω , ζ are the frequency ratio and the damping ratio, respectively, $v = \frac{\omega}{\omega_n} = \frac{f}{f_n}$, $\zeta = \frac{D}{2\omega_n H}$. If the frequency of the forced oscillation f is equal to the frequency of natural oscillation f_n and ζ is small then the amplitude of forced oscillation is large and the system is in resonance with the sine excitation.

(b) General forced oscillations

The GFO may be excited when the frequency bands of the random excitation cover the intrinsic frequencies of modes with weak damping. Thus, the input excitation is not a single frequency as SFO but a narrow band frequency. This mechanism is chosen to be applied to study the oscillations observed in real power systems [16]. Based on the stochastic linear system theory, the linear system is modeled as [17]:

$$S_y(f) = |H(f)|^2 S_u(f) \tag{3}$$

where $S_u(f)$ and $S_y(f)$ are the power spectral density (PSD) of the input stationary random process and the PSD of the output stationary random process respectively. $H(f)$ is the frequency-domain transfer function of the linear system. It's difficult to obtain an exact value of $|H(f)|^2$ in case of high-order power systems. Thus, equation (3) will be used to make a qualitative analysis. It's clear that the frequency-domain property of the system response depends on the frequency-domain property of the input random excitation and the squared amplitude-frequency property of the transfer function. For example, assuming that the power system has three oscillation modes with natural frequencies f_1, f_2 and f_3 . If the power spectral density of the input random excitation covers one mode frequency f_1 , the power spectral density of the output random excitation is very large at f_1 , and small at f_2 and f_3 as shown in Fig. 1.(a). Similarly, if the frequency band of the input random excitation changes (covers the modes with frequencies f_2 and f_3 , as shown in Fig. 1.(b), the PSD of the output variable is small at f_1 and becomes large at f_2 and f_3 . Thus, the mechanism of general forced oscillation (GFO) indicates that if the frequency bands observed in the PSD of the input random excitations cover the natural frequencies of some weaker damping modes in power systems, a forced oscillation with frequency bands around the covered mode frequencies is excited [17]. Based on the general forced oscillation mechanism, it can be speculated that if there are some random excitations in the real power system such as wind power fluctuation and its power spectral density covers the frequency of the inter-area oscillation mode, the observed oscillation is the GFO caused by this random excitation.

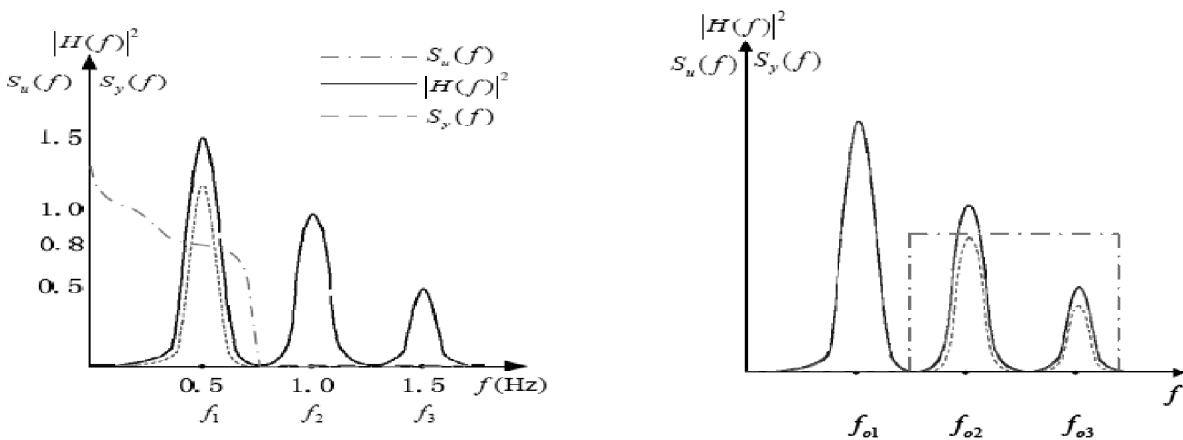


Figure 1: Principle of GFO

3. SYSTEM MODELING

3.1. Generator model

Synchronous generators are represented by a six-order model. This model is obtained assuming the presence of field circuit and an additional circuit along the d-axis and two additional circuits along the q-axis. The system has the following state variables $(\delta, \omega, e_q', e_d', e_q'', e_d'')$ and can be expressed as follows [14]:

$$\dot{\delta} = \Omega_b(\omega - 1) \tag{4}$$

$$\dot{\omega} = (P_m - P_e - D(\omega - 1))/M \tag{5}$$

$$e_q' = (-e_q' - \left(x_d - x_d' - \frac{T_{d0}'' x_d''}{T_{d0}' x_d'}(x_d - x_d')\right) i_d + (1 - \frac{T_{AA}}{T_{d0}'}) v_f^*) / T_{d0}' \tag{6}$$

$$e_d' = (-f_s(e_d') + \left(x_q - x_q' - \frac{T_{q0}'' x_q''}{T_{q0}' x_q'}(x_q - x_q')\right) i_q) / T_{q0}' \tag{7}$$

$$e_q'' = (-e_q'' + e_q' - \left(x_d' - x_d'' - \frac{T_{d0}'' x_d''}{T_{d0}' x_d'}(x_d - x_d')\right) i_d + (1 - \frac{T_{AA}}{T_{d0}'}) v_f^*) / T_{d0}'' \tag{8}$$

$$e_d'' = (-e_d'' + e_d' - \left(x_q' - x_q'' - \frac{T_{q0}'' x_q''}{T_{q0}' x_q'}(x_q - x_q')\right) i_q) / T_{q0}'' \tag{9}$$

where $x_d, x_q, x_d', x_q', x_d'', x_q''$ are the d-axis and q-axis synchronous reactance, the d-axis and q-axis transient reactance, the d-axis and the q-axis sub-transient reactance, respectively. $T_{d0}', T_{q0}', T_{d0}'', T_{q0}''$ are the d-axis and q-axis open circuit transient time constant, the d-axis and q-axis open circuit sub-transient time constant, respectively. e_d', e_q', e_d'', e_q'' are the d-axis and q-axis transient voltage, the d-axis and q-axis sub-transient voltage, respectively. ω, Ω_b, δ and M are the rotor speed, the reference speed, the rotor angle and the mechanical starting time ($2 \times$ inertia constant), respectively. P_m and P_e are mechanical power and electromechanical power.

3.2. Power system stabilizer

The power system stabilizer (PSS) uses supplementary stabilizing signals to the generator's automatic voltage regulator (AVR) reference input, to improve the dynamics performance of power systems. It's an effective method to improve the damping of the power oscillations. Inputs to the PSS are generator shaft speed, electrical power and terminal frequency. A typical PSS is shown in figure.2. It comprises two-stage phase compensation blocks, a gain block and a signal washout block. The transfer function of this PSS can be expressed as follows [18]:

$$U_i = K_{PSS} \left(\frac{sT_w}{1+sT_w} \right) \left[\frac{(1+sT_{1i})(1+sT_{2i})}{(1+sT_{3i})(1+sT_{4i})} \right] \Delta\omega_i(s) \tag{10}$$

where U_i and $\Delta\omega_i$ are the output voltage signal and the derivative of synchronous speed. The voltage signal U_i is added to the AVR reference. The signal washout block operates as a high-pass filter. It allows the signal associated with oscillations in rotor speed to pass unchanged, and it does not allow the steady state changes to modify the terminal voltages. The phase compensation block with time constants T_1, T_2 and T_3, T_4 supplies the suitable phase-lead characteristics to compensate for the phase lag between input and the output signals.

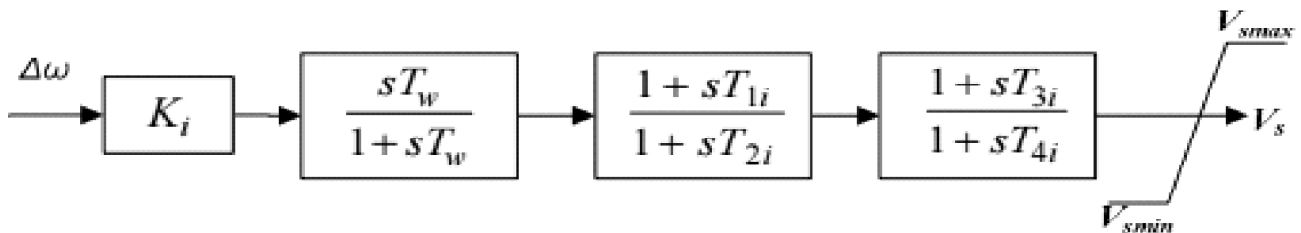


Figure 2: Structure of power system stabilizer (PSS)

3.3. DFIG Wind farm

The wind farm is composed of number of DFIG wind turbine generators aggregated on an equivalent wind turbine. The generator is modeled as a single shaft. Its dynamics can be expressed as follows [17].

$$\dot{\omega}_m = \frac{1}{2H_m}(T_m - T_e) \quad (11)$$

$$T_e = \varphi_{ds}i_{qs} - \varphi_{qs}i_{ds} \quad (12)$$

where ω_m and H_m the wind turbine speed and the inertia constant of wind turbine. Electromagnetic torque T_e and mechanical torque T_m can be calculated by:

$$T_e = x_m(i_{qr}i_{ds} - i_{dr}i_{qs}) \quad (13)$$

$$T_m = \frac{P_w}{\omega_m} = \frac{\frac{\rho}{2}c_p(\lambda)A_r v_w^2}{\omega_m} \quad (14)$$

Steady-state electrical equations of the doubly fed induction generator are assumed, as the stator and rotor flux dynamics are fast in comparison with grid dynamics, and the converter controls basically decouple the generator from the grid. As a result of these assumptions, one has:

$$v_{ds} = -r_s i_{ds} + ((x_s + x_m)i_{qs} + x_m i_{qr}) \quad (15)$$

$$v_{qs} = -r_s i_{qs} - ((x_s + x_m)i_{ds} + x_m i_{dr}) \quad (16)$$

$$v_{dr} = -r_R i_{dr} + (1 - \omega_m)((x_R + x_m)i_{qr} + x_m i_{qs}) \quad (17)$$

$$v_{qr} = -r_R i_{qr} - (1 - \omega_m)((x_R + x_m)i_{dr} + x_m i_{ds}) \quad (18)$$

where r_s the stator resistance; x_m is the magnetizing reactance; r_R is the rotor resistance; x_s is the stator reactance; x_R the rotor reactance; i_{ds} and i_{qs} are the d-axis and q-axis stator currents, respectively; v_{ds} and v_{qs} are the d-axis and q-axis stator terminal voltages, respectively; v_{dr} and v_{qr} are the d-axis and q-axis rotor voltages.

3.4. Wind Profiles

Wind speed profiles may exhibit various dynamics. In the literature different wind speed models are available, describing the ramps, the gusts and the turbulences. The main wind models namely, Weibull distribution, Mexican-Hatare cited below[14]:

a) *Weibull distribution* : It is a common way to describe the wind speed and it's modelled as follow:

$$f(v_\omega, c, k) = \frac{k}{c^k} v_\omega^{k-1} e^{-\left(\frac{v_\omega}{c}\right)^k} \quad (11)$$

where v_ω is the wind speed, c is the scale factor, it must be chosen in range of (1-10) and k is the shape factor. The time variations $v_\omega(t)$ of the wind speed are then obtained by means of a weibull distribution and expressed as follows [16]:

$$v_\omega(t) = \left(-\frac{\ln u(t)}{c}\right)^{\frac{1}{k}} \quad (12)$$

where u is a generator of random numbers and it ranges from 0 to 1.

b) *Composite wind model* : In this model the wind is composed of four components : the average and initial wind speed v_{wa} , a ramp and gust components and a turbulence. It 's expressed as follows :

$$\tilde{v}_w(t) = v_{wa}(t) + v_{wr}(t) + v_{wg}(t) + v_{wt}(t) \tag{13}$$

c) *Mexican-Hat* : This model comprises wind ramp and wind gust components. The wind ramp component can be expressed as follows:

$$t < T_{sr} : v_{wr}(t) = 0 \tag{14}$$

$$T_{sr} \leq t \leq T_{er} : v_{wr}(t) = A_{wr} \left(\frac{t - T_{sr}}{T_{er} - T_{sr}} \right) \tag{15}$$

$$t > T_{er} : v_{wr}(t) = A_{wr} \tag{16}$$

where A_{wr} is the amplitude of the wind ramp; T_{sr} and T_{er} are the starting and ending times. The wind gust component can be expressed as follows:

$$t < T_{sg} : v_{wg}(t) = 0 \tag{17}$$

$$T_{sg} \leq t \leq T_{eg} : v_{wg}(t) = \frac{A_{wg}}{2} \left(1 - \cos \left(2\pi \frac{t - T_{sg}}{T_{eg} - T_{sg}} \right) \right) \tag{18}$$

$$t > T_{eg} : v_{wg}(t) = A_{wg} \tag{19}$$

where A_{wg} is the amplitude of the wind ramp, T_{sg} and T_{eg} are the starting and ending times.

4. STUDY CASES

Our study is applied on a four-machine two areas power system [1]. It consists of two symmetrical areas linked together by two 230 kV lines of 220 km length. It was specifically designed in [1] to study low frequency electromechanical oscillations in large interconnected power systems. Each area comprises two identical round rotor generators rated 20 kV/900 MVA. The synchronous generators are presented by a six-order model with magnetic saturation neglected and voltage regulators and they have identical parameters. There is 2800MW installed generation capacity in this system (1400 MW in each area), and 400 MW of the total active power is transmitted from area 1 to area 2. We connect a DFIG wind farm at the sending end of area 1 at bus 6. The penetration level is 10% of the total installed active power of area 1 (140 MW). The test system is shown in Figure 3. Simulation results were carried out using a Power System Analysis Toolbox (PSAT) [16], which is a MATLAB-based toolbox for power system studies. Table 1 presents the study cases.

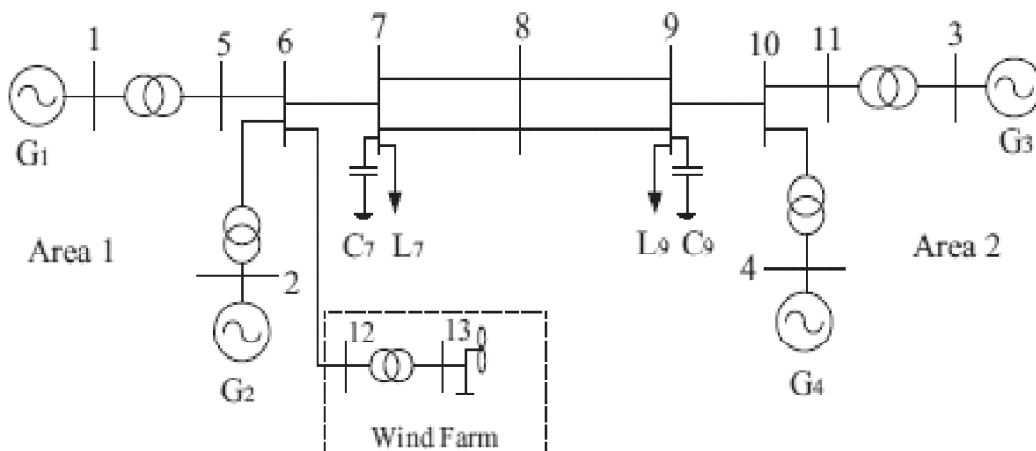


Figure 3: Four-machine two areas power system with wind farm

Table 1
Study cases

<i>Cases/wind Profiles</i>		<i>Linear modal analysis</i>	<i>Frequency domain analysis</i>
No WTG	No PSS	X	-
	PSS	X	-
Weibull	No PSS	X	X
	PSS	X	-
Mexican-hat	No PSS	X	X
	PSS	X	-
Composite	No PSS	X	X
	PSS	X	-

5. SIMULATION RESULTS

5.1. Linear modal analysis

We perform linear modal analysis to assess the resulting oscillation modes for different cases. Table 1 summarizes the results. It can be noticed that without wind farm there are two local modes and one inter-area mode:

- Local mode 1: oscillations of G1 against G2 in area 1.
- Local mode 2: oscillations of G3 against G4 in area 2.
- Inter-area mode 1: oscillations of generators in area 1 against generators in area 2.

The integration of the DFIG wind farm induced another inter-area oscillation mode. Its frequency depends on the wind profile, as depicted in Figure 4. We note that for the cases of Weibull and Mexican wind speed profiles, the new inter area mode frequencies are around 0.16 Hz, whereas in the case of Composite wind model, the frequency was slightly higher, namely about 0.23 Hz. However, the frequency of the existing inter-area mode is practically unchanged. On the other hand, the damping ratio of the induced inter-area mode depends on the wind profile: For the composite wind model, the damping ratio was lower.

Table 2
Resulting electromechanical oscillations

<i>Case/Wind profiles</i>	<i>Modes</i>	<i>Eigenvalue (λ)</i>	<i>Damping ratio ζ(%)</i>	<i>f(Hz)</i>
No wind farm	Local mode 1	-0.8213i 6.523	12.5	1.0464
	Local mode 2	-1.1116i 6.1282	17.84	0.99125
	Inter-area mode	-0.20754i 3.7044	5.6	0.5905
Weibull distribution	Local mode 1	-0.97637i 6.4187	15.02	1.0333
	Local mode 2	-1.0949i 6.0955	17.67	0.98565
	Inter-area mode 1	-0.23091i 3.56	6.47	0.5677
	Inter-area mode 2	-0.27856i 0.96041	27.85	0.15915
Mexican HAT	Local mode 1	-0.97637i 6.4187	15.02	1.0333
	Local mode 2	-1.0955i 6.0955	17.69	0.98558
	Inter-area mode 1	-0.23116i 3.5621	6.47	0.56811
	Inter-area mode 2	-0.27891i 0.9741	27.53	0.16126
Composite wind model	Local mode 1	-0.97637i 6.4187	15.02	1.0333
	Local mode 2	-1.0998i 6.094	17.76	0.98555
	Inter-area mode 1	-0.23601i 3.656	6.44	0.58308
	Inter-area mode 2	-0.25156i 1.4141	17.51	0.22859

Given that the power wind fluctuations are considered as random excitations, we use the general forced oscillation mechanism (GFO) to explain the obtained results. Since the GFO is investigated in frequency domain, we use the power spectral density to convert wind power from the time domain into the frequency domain. The PSD indicates how the wind power is distributed over the different frequencies. If the narrow frequency band of the wind power output covers the natural oscillation frequencies of the power system, then, a forced oscillation with frequency bands around the covered frequencies would be excited [13], and we can consider that the new inter area mode indicated by modal analysis is induced by the wind farm.

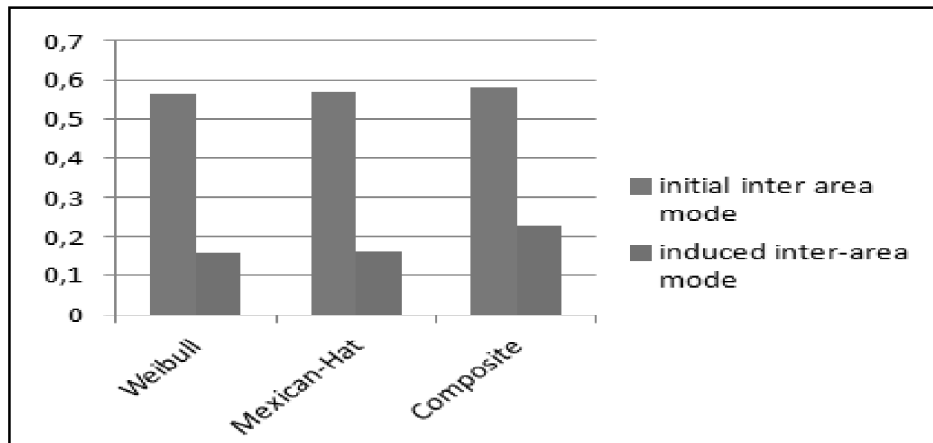


Figure 4: Frequencies of inter-area oscillation modes for different wind speed profiles

5.2. Frequency domain analysis

We apply the PSD on the output power of the DFIG wind farm for different wind speed profiles. The wind power generated from the wind farm for different wind speed profiles and their respective PSD are illustrated by figures 5-10. It can be seen from figures 6, 8 and 10 that the wind power generated by the DFIG wind farm is distributed on a frequency band, which depends on wind speed profiles. The dominant frequency band ranges from 0.1 Hz to 0.2 Hz in the case of Weibull distribution. In the case of Mexican-hat, the dominant frequency band is ranging from (0.01 Hz to 0.4 Hz). And in the case of composite wind profile, this band is [0.15 -0.25 Hz]. On the other hand, the modal analysis indicates that the frequency of the new inter-area mode is approximately 0.16 Hz in the two first cases and 0.22 Hz in the case of composite wind profile. It's clear that the frequency band observed in the PSD of the wind power output covers the frequency of the inter-area mode. Therefore, the wind power fluctuation can be regarded as a narrow-band random excitation of inter-area oscillations in power in interconnected power system. For the different cases, the PSD of the wind power generation covers the frequency of the induced inter-area mode. So, based on the mechanism of general forced oscillation, wind power fluctuations may be considered as an excitation source of power oscillations and the induced inter-area mode can be considered as the GFO caused by the wind power fluctuations.

5.3. Power system stabilizer performances

A typical power system stabilizer (PSS) represented by a gain K_{PSS} , a two lead/lag blocks and a washout block is added to each generator of the test system. The purpose is to evaluate their performances in damping the various excited inter-area oscillations, in particular those excited by the wind power. The parameters of the PSS are tuned as in [1] assuring damping of the natural oscillation mode of the system. Table 3 summarizes the modal analysis results of the system with and without PSS, for the different wind profiles: Weibull distribution, Mexican HAT and Composite wind model. The comparison between the damping of the new inter area mode for different wind profiles is illustrated in figure 10.

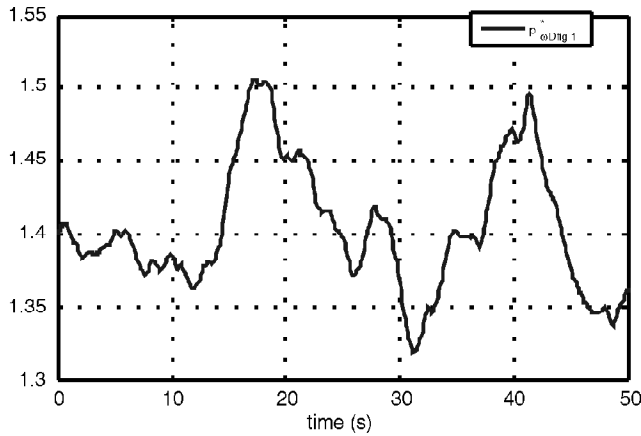


Figure 5: Wind power output in the case of weibull distribution

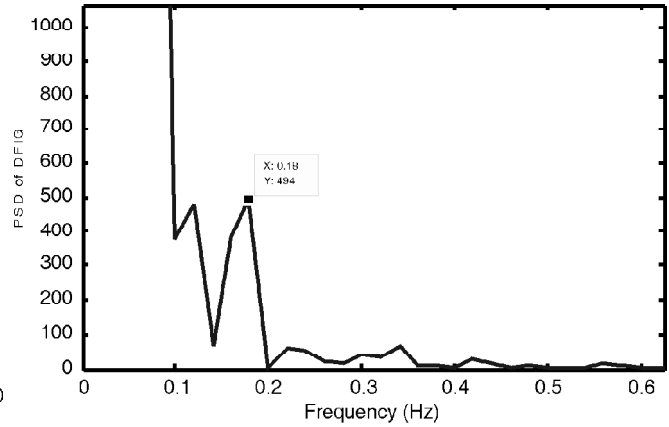


Figure 6: PSD of the Wind power output in the case of weibull distribution

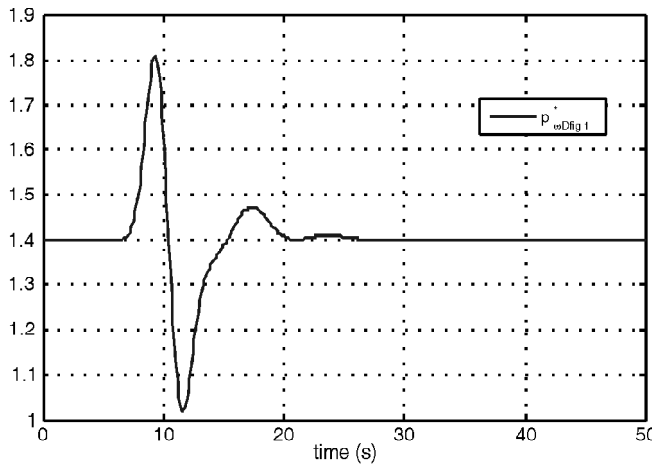


Figure 7: Wind power output in the case of Mexican-hat profile

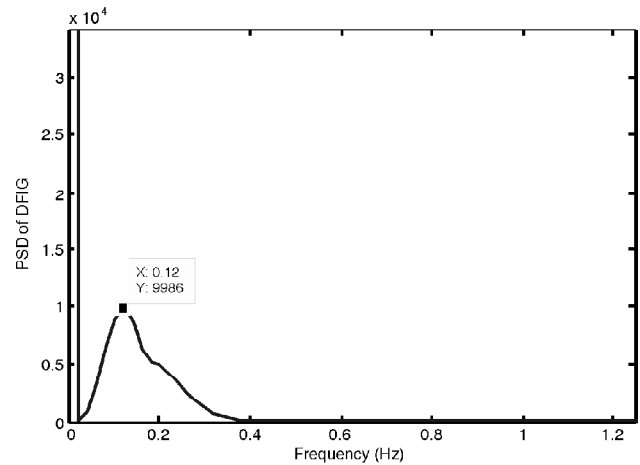


Figure 8: PSD of the Wind power output in the case of Mexican-hat profile

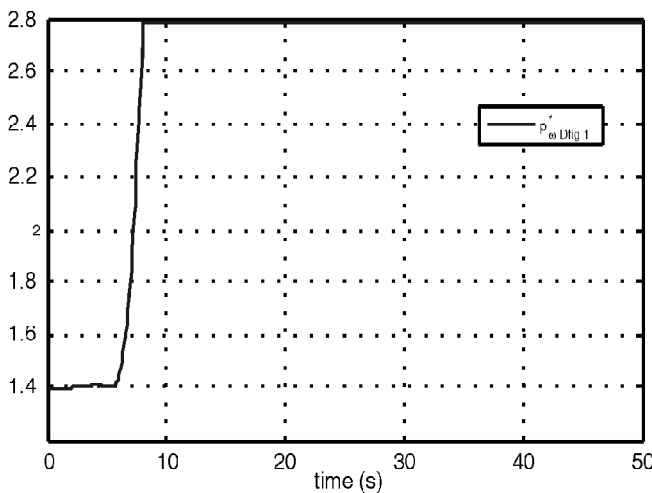


Figure 9: Wind power output in the case of Composite profile

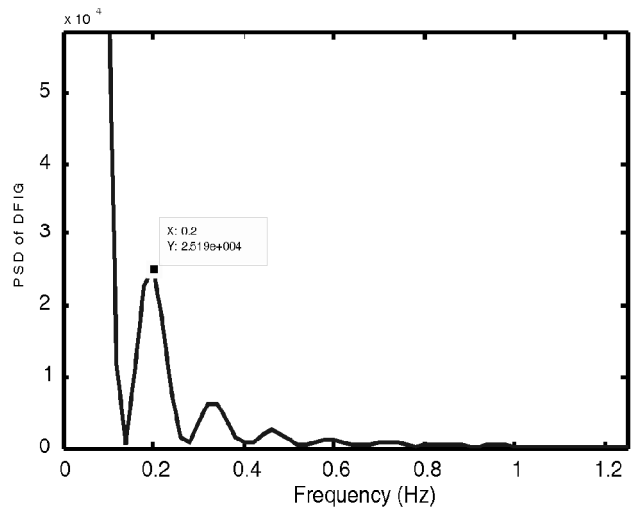


Figure 10: PSD of the Wind power output in the case of Composite profile

Table 3
Modal analysis results with and without PSS

Case/Wind profiles		Modes	(%)	$f(\text{Hz})$
No wind farm	No PSS	Inter-area mode 1	5.6	0.5905
	PSS	Inter-area mode 1	21.35	0.59266
Weibull distribution	No PSS	Inter-area mode 1	6.47	0.5677
		Inter-area mode 2	27.85	0.15915
	PSS	Inter-area mode 1	21.67	0.57161
		Inter-area mode 2	61.83	0.17222
Mexican HAT	No PSS	Inter-area mode 1	6.47	0.56811
		Inter-area mode 2	27.53	0.16126
	PSS	Inter-area mode 1	21.66	0.57167
		Inter-area mode 2	61.93	0.17143
Composite wind model	No PSS	Inter-area mode 1	6.44	0.58308
		Inter-area mode 2	17.51	0.22859
	PSS	Inter-area mode 1	21.44	0.58517
		Inter-area mode 2	40.84	0.22674

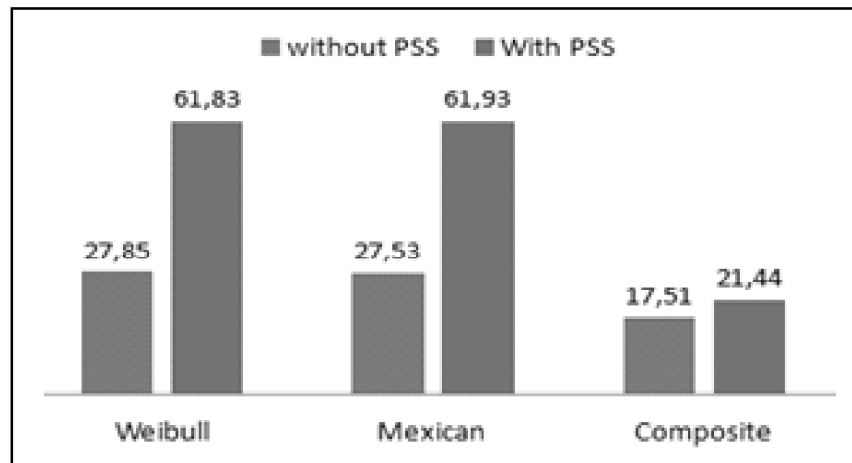


Figure 11: Damping of induced inter area oscillation mode for different wind speed profiles

From Table 3, it can be noticed that the PSS improves the damping of the existing and the induced inter area modes. Thus, the conventional PSS if it is well tuned, it can improve the damping of the forced oscillations in power systems. From figure 11, it's clear that the damping of the induced inter-area mode and the performances of PSS depends on the wind speed profile. Indeed, the lowest damping is in the case of the composite model.

5. CONCLUSIONS

This paper has investigated the issue of inter-area oscillations induced by wind power fluctuations and their control by standard power system stabilizers. First, we demonstrated that specific wind speed profiles may induce inter-area oscillations as a general forced oscillation mechanism. Second, performances of power system stabilizer (PSS) were assessed for the control and the damping of the wind induced oscillations. The wind power output was frequency-analyzed by the power spectral density (PSD) and the general forced oscillation mechanism

is used in search for a correlation between the wind power spectrum and the inter-area oscillation frequencies indicated by modal analysis. The study was applied on a four-machine two areas power system.

The power spectral density analysis indicated that wind power is distributed on a narrow frequency band. This band depends on the wind speed profile. This frequency band covers the frequency of the induced inter-area oscillation mode indicated by linear modal analysis. Thus, the induced inter area mode may be the general forced oscillation caused by wind power fluctuations. From the control point of view, it was shown that the PSS improved the damping of the excited inter area mode, which was more prominent for the weibull wind profile and less for the composite wind model. PSS parameters should be further optimized for different system operating conditions and wind penetration levels

REFERENCES

- [1] P. Kundur, *Power System Stability and Control*, New York: McGraw-Hill; 1994.
- [2] F. Berrutti, Á. Giusto, and M. Arstein, "Impact of variable speed wind on power system oscillations". 2013 IEEE Power and Energy Society General Meeting, 2013.
- [3] A.E. Leon and J.A. Solsona, "Power oscillation damping improvement by adding multiple wind farms to wide-area coordinating controls". *IEEE Transactions on Power Systems*, 29 (3), 1356-1364, 2014.
- [4] K. Kim, H. Schattler, J. Zaborszky, V. Venkatasubramanian and P. Hirsch, "Methods for calculating oscillations in large scale power systems". *IEEE Transactions on Power Systems*, 12, 1639-1648, 1997.
- [5] K.R. Rao and L. Jenkins, "Studies on power systems that are subjected to cyclic loads". *IEEE Transactions on Power Systems*, 3, 31-37, 1988.
- [6] Y. Yu, Y. Min, L. Chen, and P. Ju, "The disturbance source identification of forced power oscillation caused by continuous cyclical load." In Proceedings of the International Conference on Electric Utility Deregulation and Restructuring and Power Technologies (DRPT), Weihai, China, July 6-9, pp. 308-313, 2011.
- [7] Z.X. Han, Z.L. Zhu, X.S. Tian and F. Li, "Analysis and simulation research on power system low frequency oscillation." In Proceedings of the International Conference on Computer Modeling and Simulation (ICCMS), Sanya, China, Jan. 22-24, pp. 223-228, 2010.
- [8] O.H. Souza, N. Barbieri, and A.H.M. Santos, "Study of hydraulic transients in hydropower plants through simulation of nonlinear model of penstock and hydraulic turbine model." *IEEE Trans. Power Syst.* 14, 1269-1272, 1999.
- [9] Y.F. Liu, P. Ju, F. Wu, Y.P. Yu, and J.Y. Zhang, "Computation comparisons of power system dynamics under random excitation". In Proceedings of the IEEE PowerCon, Chengdu, China, Oct. 20-22, pp. 752-758, 2014.
- [10] M. Jafarian, and A.M. Ranjbar, "Interaction of the dynamics of doubly fed wind generators with power system electromechanical oscillations," *IET Renew. Power Gener.*, 7, 88-97, 2013.
- [11] Liu, Y.L.; Yu, Y.X. Transient stability probability of a power system incorporating a wind farm. *Sci. China Tech. Sci.* **2016**, 59, 973-979.
- [12] S. Brownlee, D. Flynn, B. Fox, and T. Littler, "The impact of wind farm power oscillations on the Irish power system." In Proceedings of the IEEE PowerTech, Lausanne Switzerland, July 1-5 (PowerTech-2007), pp. 195-200, 2007.
- [13] J. Ping, L. Yongfei, F. Wu, F. Dai and Y. Yu, "General forced oscillations in a real power grid integrated with large scale wind power energies," *Energies*, 9 (7), Article ID 525, July 2016.
- [14] F. Milano, *Power System Analysis Toolbox*, Documentation for PSAT version 2.1.9, July 14, 2005, available on www.power.uwaterloo.ca
- [15] Y. Liu, P. Ju, J. Chen, Y. Zhang, and Y. Yu, "Contrastive analysis of general and special forced oscillations of power systems." *CSEE J. Power Energy Syst.* 1, 61-68, 2015.
- [16] D.E. Newland, *An Introduction to Random Vibrations: Spectral & Wavelet Analysis*, 3rd edition, Longman Inc.: New York, NY, USA, 1993.

- [17] N. Ikram, K.B. Kilani and M. Elluech, "Impact of wind turbine generators on low frequency oscillations in power systems." CISTEM-2016 Conference Proceedings, 2016.
- [18] E. Mahdiyeh, H. Shareef and A. Mohamed,"Optimal tuning of power system stabilizers using modified particle swarm optimization."Middle East Power Systems Conference (MEPCON), 2010.
- [19] Y. Tang, "Fundamental theory of forced power oscillation in powersystem," *Power System Technology*, 30 (10), 29-33, May2006.
- [20] A.T. Azar and S. Vaidyanathan, *Chaos Modeling and Control Systems Design*, Springer, Berlin, 2015.
- [21] S. Vaidyanathan and C. Volos, *Advances in Memristors, Memristive Devices and Systems*, Springer, Berlin, 2017.
- [22] S. Vaidyanathan and C.H. Lien, *Applications of Sliding Mode Control in Science and Engineering*, Springer, Berlin, 2017.
- [23] S. Vaidyanathan, "A novel 3-D conservative chaotic system with sinusoidal nonlinearity and its adaptive control", *International Journal of Control Theory and Applications*, 9 (1), 115-132, 2016.
- [24] S. Vaidyanathan and S. Pakiriswamy, "A five-term 3-D novel conservative chaotic system and its generalized projective synchronization via adaptive control method", *International Journal of Control Theory and Applications*, 9 (1), 61-78, 2016.
- [25] V.T. Pham, S. Jafari, C. Volos, A. Giakoumis, S. Vaidyanathan and T. Kapitaniak, "A chaotic system with equilibria located on the rounded square loop and its circuit implementation," *IEEE Transactions on Circuits and Systems-II: Express Briefs*, 63 (9), 2016.
- [26] S. Vaidyanathan and S. Sampath, "Anti-synchronisation of identical chaotic systems via novel sliding control and its application to a novel chaotic system," *International Journal of Modelling, Identification and Control*, 27 (1), 3-13, 2017.
- [27] S. Vaidyanathan, K. Madhavan and B.A. Idowu, "Backstepping control design for the adaptive stabilization and synchronization of the Pandey jerk chaotic system with unknown parameters," *International Journal of Control Theory and Applications*, 9 (1), 299-319, 2016.
- [28] R.K. Goyal, S. Kaushal and S. Vaidyanathan, "Fuzzy AHP for control of data transmission by network selection in heterogeneous wireless networks," *International Journal of Control Theory and Applications*, 9 (1), 133-140, 2016.
- [29] C.K. Volos, D. Prousalis, I.M. Kyprianidis, I. Stouboulos, S. Vaidyanathan and V.T. Pham, "Synchronization and anti-synchronization of coupled Hindmarsh-Rose neuron models," *International Journal of Control Theory and Applications*, 9 (1), 101-114, 2016.
- [30] S.M.B. Mansour and V. Sundarapandian, "Design and control with improved predictive algorithm for obstacles detection for two wheeled mobile robot navigation," *International Journal of Control Theory and Applications*, 9 (38), 37-54, 2016.